# Chapter 1

# Introduction

Energy is needed to sustain life. Nowadays, mankind requires energy not only for food, but also for making life more comfortable. The high demand of energy needed to maintain our living standards is constantly increasing. To tackle this growing challenge, new solutions for sustainable energy sources have to be explored. Nearly all life on earth is based either directly or indirectly on solar energy. This form of energy is abundantly available. Plants convert the electromagnetic energy from the sun to chemical energy using photosynthesis [1]. However, this is not the only way to harness solar energy. It can be used to heat up material as thermal energy, or be converted to electric energy. Regarding potential applications, electric energy is much more versatile. The direct conversion of electromagnetic radiation to electricity is called photovoltaics. It is the artificial analogon to photosynthesis [2]. The photovoltaic effect was first discovered in 1839 by M. E. Bequerel [3], the first practical photovoltaic cell was prepared at Bell laboratories with an efficiency of 4.5% in 1953 [4]. Since the first launch of a solar-powered satellite in 1958 (Vanguard I satellite [5]), research progressed quickly. Today, the most efficient but also most expensive solar cells are still used to power satellites. For commercialization on earth, a decrease in cost as compared with space applications is necessary in order to make the solar

energy an affordable alternative to non-sustainable energy production, even if the efficiency is lower compared to space applications.

Typical solar cell technologies are based on inorganic materials like crystalline silicon [4]. Even though crystalline silicon cells are the standard of today's photovoltaics technology, these cells face several disadvantages. The silicon based cells require a lot of material and also need complicated and expensive preparation steps. Thin film solar cells that require less material are also possible, based for example on cadmium telluride (CdTe), copper indium gallium selenide (CIGS) or amorphous silicon (a-Si). Even though they require less material, the material is still expensive. In the case of CdTe and CIGS, some of the used materials are even toxic. A further drawback is the mechanical inflexibility of the inorganic cells, which limits the possible range of applications. In addition to the inorganic materials, novel materials based on organics are also investigated for use in photovoltaics. This research was triggered by the discovery of conducting polymers via oxidative doping in the 1970s [6]. With the award of the Nobel prize in chemistry in 2000 [7], organic semiconductors finally gained broad attention in research and industry and have since been investigated extensively and are already applied commercially today. All-organic solar cells are highly promising candidates for alternatives to their inorganic counterparts. The required material is potentially cheap to fabricate, only very small amounts of the materials are required, and the production routes require less money and energy. A novel class of solar cells, which is investigated in the present thesis, combines the advantages of both inorganic and organic materials. This class of solar cells comprises the so-called hybrid and the solid-state dye-sensitized solar cells (ssDSSCs). These cells are based on an inorganic electron conducting material - in case of ssDSSCs with the addition of a dye - combined with an organic hole-conducting material. Typical inorganic materials used in these cells are metal oxides, for example titania which is a low-cost material and abundantly available. These are crucial prerequisites, since they should not contradict the advantages of organic semiconductors as listed above.

The principle operating mechanism of a solar cell includes the following three steps: one, the absorption of light and excitation of charges, two, the separation of the charges and three, the conduction of electrons and blocking of holes on one side, and the conduction of holes and blocking of electrons at the other side of the cell [2, 8]. In the inorganic solar cells, the charge separation occurs at pn-junctions in layered structures. For organic and also the hybrid solar cells and ssDSSCs, the interface between two materials provides the energy necessary for the separation of the charges. In the case of all-organic solar cells, the most efficient structure consists of a so-called bulk heterojunction (BHJ), where both electron- and hole-conducting materials build up intermixed phases in a blend [9, 10]. Likewise, for the hybrid photovoltaics and ssDSSCs, it is essential to have controlled titania nanostructures. The preparation of titania nanostructures in general is possible through various production routes [11]. One possible way to fabricate titania is via sol-gel synthesis, which is a wet-chemical process and thereby offers various possibilities of film preparation, including printing techniques. Polymer templates, for example comprised of block copolymers, are a powerful tool to control inorganic nanostructures. The combination of sol-gel synthesis and block copolymer templates, which is used in the presented work, is very promising, especially for applications in energy conversion and storage [12].

In the presented thesis, the investigations focus on how the structure of the films is related to their functionality. The understanding of this most basic principle is crucial for solar cells that depend on the nanostructure, as in the case of organic solar cells [13]. However, gaining access to this information is highly challenging since most of the reactions occur inside the active films and are not directly accessible with standard imaging techniques. Therefore, the investigation techniques include comprehensive scattering investigations to understand the morphology on the scale of a solar cell device.

A sketch summarizes all the different aspects on the route from controlling the structure of titania films to the complete solar cell (figure 1.1). All questions tackled in the present thesis are related to the photo-

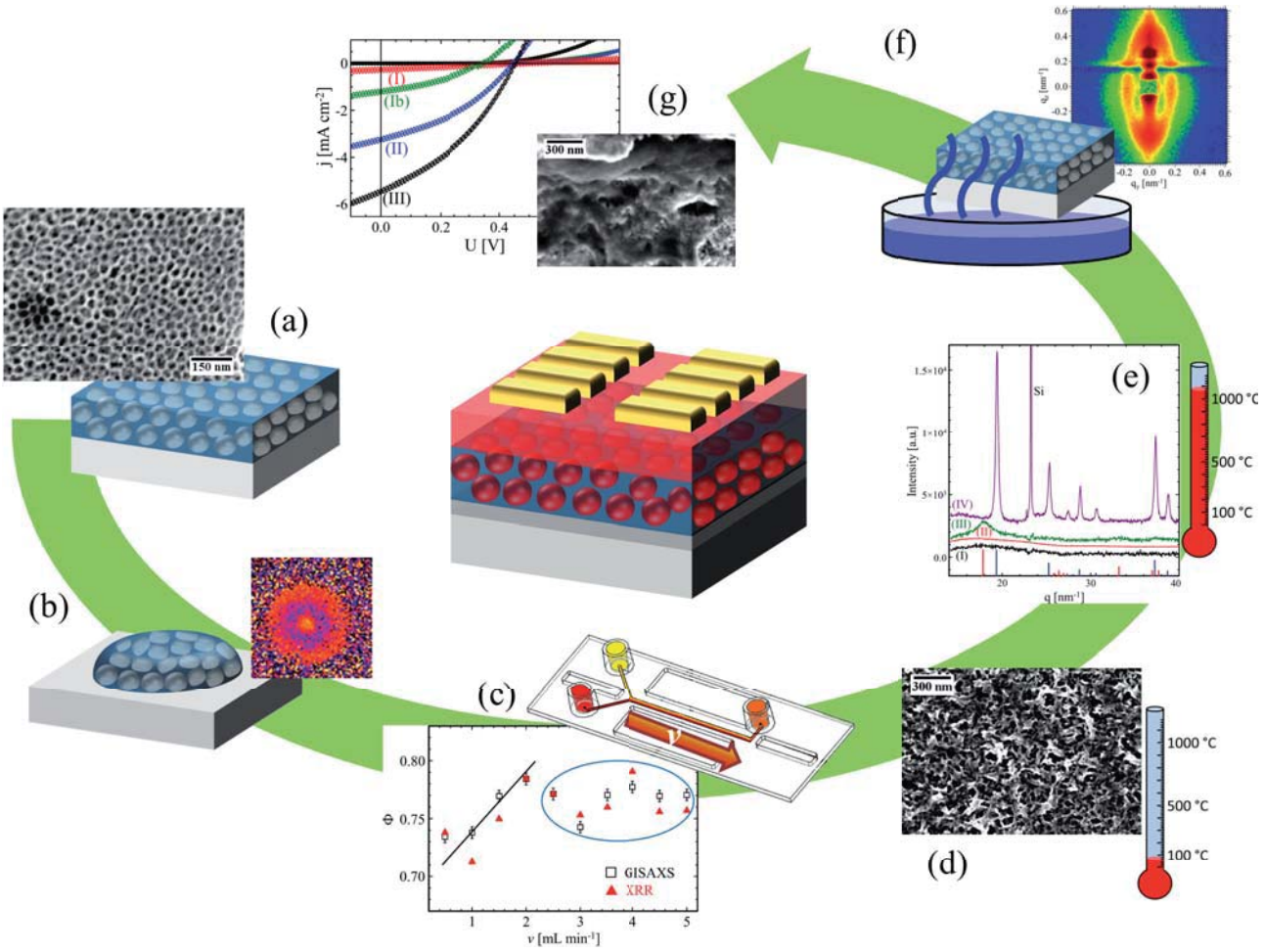


**Figure 1.1:** Overview: the different questions tackled in the present thesis include aspects of hybrid and solid-state dye-sensitized solar cells, as sketched in the center of the illustration. The aspects comprise the control of titania nanostructures (a), both in thin films and in a structured drop (b), and possible improvement of the structures with micro-fluidics (c). The influence of synthesis temperature, both for structuring at low temperatures (d) and at higher temperatures (e), and the stability of the resulting nanostructured films in water vapor (f) are also investigated. The whole stack of solar cells is probed as well (g), with a focus on the influence of different filling techniques of the titania nanostructures with hole-conducting materials.

voltaic device. As noted above, the combination of sol-gel synthesis with structure-directing block copolymers allows for the structuring of titania thin films. When aiming for industrial application, drop-like structures

as from ink-jet printing are of huge importance. This leads to the question: how do the structures differ in a homogeneous thin film from the structures in a drop of titania? Furthermore, typical nanostructured titania films do not show a high degree of order. The question is addressed, whether it is possible to improve the resulting titania nanostructure by a control of the mixing of the sol-gel components by the application of micro-fluidics. Crystallinity is a critical aspect of the conductivity, which is important for solar cell applications. Usually, crystallinity is obtained through high temperature treatments. When aiming for the production of solar cells on flexible substrates, that would allow for roll-to-roll printing, the synthesis needs to take place at temperatures which are sufficiently low. The question arises whether it is possible to control titania nanostructures prepared at low temperatures with a high degree of crystallinity. On the route to the complete solar cell, the titania nanostructures need to be filled with dye and hole-conducting materials. How does the titania structure and the crystallinity change with different high temperature treatments, and how stable are the titania nanostructures against capillary pressure when filling, for example, with water vapor? Furthermore, the question is posed of how the titania nanostructures can be filled with hole-conducting materials. What is the most efficient pathway for the filling and how is the resulting solar cell efficiency affected?

In order to tackle all these important questions on the route to solar cells prepared from the combination of inorganic and organic materials, the thesis is structured as follows. To provide the basis to discuss the investigations, the theoretical basics in chapter 2 include solar cell basics, notes on polymer theory, titania theory and also on scattering theory, which is important for the structure investigations. Chapter 3 briefly introduces the methods for characterization of both, functionality and structure of the investigated systems. The sample preparation is described in chapter 4 with a focus on its basics. Specifics of the investigated samples are given in the corresponding chapters along with discussion of results. The question of the titania nanostructures is tackled in chapter 5, both in thin film and in a drop, as well as possible

improvements with micro-fluidics. A possible low temperature synthesis route of titania nanostructures is investigated in chapter 6. Changes in dependence of high temperature treatments are discussed in chapter 7, with an investigation of calcination settings and the probing of mechanical stability against infiltration with water vapor. The degree of filling of titania structures with a hole-conducting material and the resulting solar cell efficiencies are investigated in chapter 8. In the summary and outlook in chapter 9, the answers to the above posed questions are given as they are obtained in the present investigations.

# Chapter 2

# Theoretical aspects

The investigated systems are used for solar cells of novel type. The functionality of the solar cells is correlated with structural properties. The goal is to understand structure formation and functionality of titania-based solar cells. The different involved theoretical concepts are presented in the present chapter, from the solar cell principles in section 2.1 to polymer basics in section 2.2, which are necessary for both parts of the active material, hole- and electron-conductor, to the basics of the electron-conductor titania in section 2.3. Furthermore, scattering investigations are a crucial aspect to investigate the morphology in the thin film volume, the basics thereof are discussed in section 2.4, tomography basics in section 2.5.

The basic principles of solar cells are presented (section 2.1.1) as well as the two different types of titania-based solar cells, hybrid solar cells (section 2.1.2) and solid-state dye-sensitized solar cells (section 2.1.3). The polymer basics of block copolymers (section 2.2.1) and conducting polymers (section 2.2.2) are explained, as they are necessary for the understanding of titania structure templating with block copolymers and for the setup of the solar cells with conducting polymers. The basic titania properties, including the different crystal phases and semiconducting properties, are explained in section 2.3.1, the basics of the sol-gel synthesis (section 2.3.2) and the basics of the combination of sol-gel synthesis

with structure-directing block copolymers (section 2.3.3) are introduced subsequently. For the structure investigations, scattering investigations play a major role. The basics of scattering are discussed along with the theoretical basics of reflectivity (section 2.4.1), diffraction (section 2.4.2) and grazing incidence scattering (section 2.4.3), including a discussion of the scattering contrast, the Yoneda peak, the time-of-flight (TOF) mode, notes on fitting and depth information. Furthermore, the basics of tomography investigations are discussed in section 2.5, with a special focus on GISAXS tomography.

## 2.1 Solar cells

Solar cells or photovoltaic cells in general encompass all electronic devices that convert electromagnetic energy (from solar light, infrared, visible and ultraviolet) to electrical energy. The main processes always include the absorption of light, creation of free charge carriers and the transport of the charge carriers to two electrodes that are to be contacted [8]. The materials that are responsible for these three main processes are called active materials. In principle, a lot of different materials, solid and liquid, are used as active materials in solar cells. In the present investigation, the focus lies on titania based solar cells. Titania participates in the charge separation and acts as the electron-conductor in these systems. Two significantly different concepts exist for this class of solar cells. On the one hand, the hybrid solar cells combine titania with a hole-conducting material. Dye-sensitized solar cells (DSSCs) on the other hand use an additional dye layer between titania and the hole-conductor. Both concepts are discussed in the following, after the introduction to the basic principles involved in solar cell devices.

### 2.1.1 Basic principles

Solar cells based on titania use a multilayer stack built up, the principle setup is shown as a sketch in figure 2.1 along with the most important involved layers. The incoming light has an energy of $E = h\nu$, where $h$

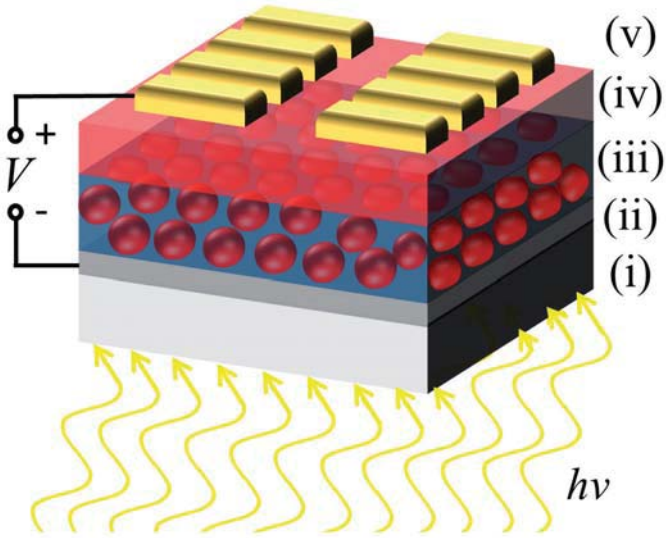


**Figure 2.1:** Basic setup of a solar cell based on titania: the light with energy $h\nu$ enters through the transparent substrate (i), depicted in light gray, covered with the transparent cathode (ii), depicted in dark gray. The active material consists of the electron conductor (iii), depicted in dark blue, and a hole-conductor (iv), depicted in red. The gold electrodes reside on top (v), illustrated in yellow.

is Planck's constant and $\nu$ is the frequency of the light. The transparent electrode on top of the transparent substrate (glass or foil) typically consists of transparent conductive oxides (TCOs) like fluorine-doped tin oxide (FTO) or indium-doped tin oxide (ITO), but graphene or carbon nanotubes can also be used. The top electrode usually is a metal layer. Between the two electrodes, the active layer is present where the photovoltaic processes happen. In the case of hybrid solar cells, an electron-conducting material like titania and a hole-conducting material constitute the active layer. In the case of solid-state dye-sensitized solar cells (ssDSSCs), a monolayer of dye covers the titania surface, and a solid hole-conductor completes the active material.

The principle processes involved in the transformation of solar energy to electrical energy are depicted schematically in figure 2.2. For the creation of charge carriers, light with an energy $h\nu$ is absorbed (figure 2.2(a)). The absorption leads to the excitation of the charges in the absorbing material, which consists either of the hole-conducting polymer in the case of hybrid solar cells or the dye in ssDSSCs. By the excitation, bound electron-hole pairs form, which are called excitons. The binding energy of the excitons in the investigated hybrid systems is rather high with typically around 0.5 eV [14]. Therefore, the excitons cannot be split by the thermal energy, which is of the order of several

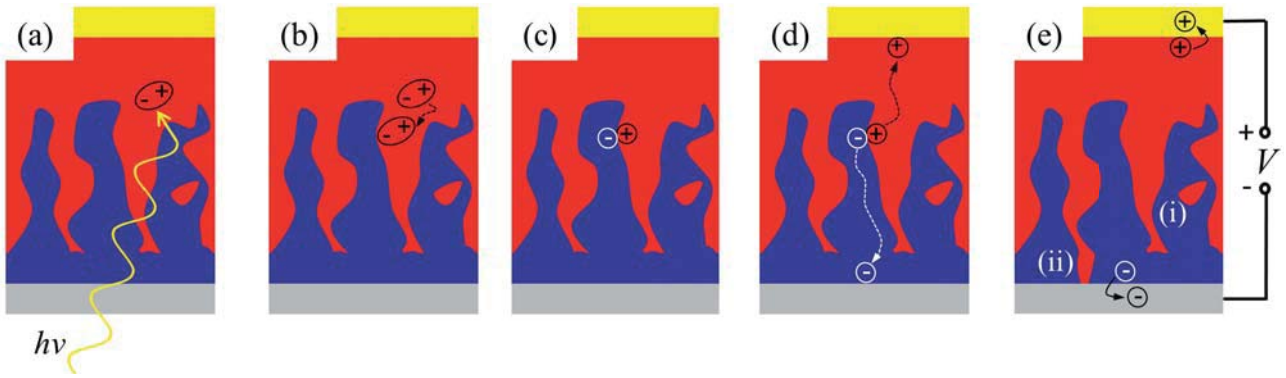


**Figure 2.2:** Principle processes in solar cell: the schematic illustration shows the active material, consisting of the electron conductor in dark blue and the hole-conductor in red between the top electrode (yellow, anode) and the bottom electrode (dark gray, cathode). For the creation of charge carriers, light with an energy $h\nu$ is absorbed (a) and creates excitons. The excitons diffuse to an interface (b) in the case of hybrid solar cells. In the case of dye-sensitized solar cells, the absorption occurs in the dye molecules which are directly located at the interface. In the next step, the excitons dissociate (c) and separate charges are obtained. After charge transport (d), the charges are extracted at the respective electrodes (e) and recombine through an external circuit. Losses through recombination can occur in parts of the materials with no connecting pathway to the electrode (i) and at contact of the materials to the wrong electrode (ii).

meV. The next important process is consequently the diffusion of the exciton to an interface of the electron- and the hole-conducting material (figure 2.2(b)). In the case of ssDSSCs, the absorption occurs in the dye molecules which are located directly at the interface to titania [15]. Therefore, no diffusion of the excitons occurs for that type of solar cells. At the interface, the exciton can be split and charges are separated (figure 2.2(c)). After charge separation, the electrons and the holes have to be conducted to the cathode and the anode, respectively (figure 2.2(d)). At the electrodes, the charges are extracted, and can recombine through an external circuit (figure 2.2(e)).

The absorption and the charge separation are different for the two different types of investigated solar cells, hybrid solar cells and ssDSSCs.

Due to their importance and the resulting main differences in the different types of solar cells, the absorption and charge separation processes are discussed for the different types of solar cells separately in the following (sections 2.1.2 and 2.1.3). Furthermore, details on excitons are given there as well.

The charge transport is a property of the respective materials. Therefore, the conduction of holes in a hole-conducting polymer is discussed in section 2.2.2 along with the properties of polymers. The conduction of electrons in titania is discussed along with other titania properties in section 2.3.1.

The charge extraction and the following recombination through an external circuit depend on the combination of materials and on the device architecture. The most important aspect of the charge extraction at the bottom electrode is that electrons have to be exchanged reversibly and holes need to be blocked. For this purpose, a low work function (the energy difference between the Fermi level in the material and the vacuum state) of the electrode material is necessary [16]. At the top electrode, in contrast, the exchange of holes needs to be reversible and the blocking of electrons needs to be ensured, which is best accomplished with a metal contact with a high work function. For the blocking of the opposite charges, compact layers of titania at the bottom electrode and of the hole-conductor near the top electrodes are applied, respectively.

The efficiency is limited mainly by three properties, recombination processes of excitons before separation in the case of hybrid solar cells, recombination of separated charges, and incomplete filling of pores and consequent incomplete charge separation. Separated charges cannot be extracted and recombine either in case of an inclusion with no interconnected pathway to the corresponding electrode or when in contact with the opposite electrode. These two charge recombination scenarios are depicted exemplary in figure 2.2(e) by the island (i) and the contact (ii) for the bottom electrode. Interpercolating pathways and compact layers at the electrodes are necessary to prevent the recombination mechanisms.

A special aspect of the incomplete charge separation results from the typical production of the solar cells. As the titania nanostructure

is usually prepared before the filling with the hole-conducting material, incomplete filling of the titania nanostructure with the hole-conducting material results in a limited solar cell efficiency and is among the most important aspects for increasing the efficiency [17, 18, 19]. The theory of the wetting of nanostructures with a liquid like the polymer or dye solution is still not understood completely even in the case of regular structures like nanotubes [20]. The wetting of a liquid drop on a substrate is described by a modification of Young's equation

$$\gamma_{\text{liquid-vapor}} \cos(\beta) = \gamma_{\text{solid-vapor}} - \gamma_{\text{solid-liquid}} - \tau\kappa \tag{2.1}$$

with the surface tension $\gamma_{\text{a-b}}$ between the phase $a$ and $b$. $\beta$ is the contact angle of the drop relative to the surface. $\tau$ is the line of tension of the triple line and $\kappa$ the curvature of said line. Figure 2.3 illustrates both a drop on a surface and confined within a channel. In the case of a circular drop with radius $R$, the curvature $\kappa = R$. Equation (2.1) also holds for nanometer sized droplets, and any surface roughness is included via $\tau$ as well. But the extension of the theory to nanochannels is not conclusive so far. Furthermore, in many cases a liquid monolayer is adsorbed on the surface of nanochannels before the drop, which deforms the meniscus profile. For sizes below a critical size, the continuum model no longer applies, but this border is typically of the order of 2 nm [21]. For larger structures, the continuum model can be used to calculate the contact angle between liquid and solid, albeit the angle is different for confinement inside a nanotube than on top of a flat surface. Furthermore, a thermodynamic approach has shown that in porous structures, the structures are filled from the smaller to the larger structures [22]. In case of the filling of a mesoporous structure with water vapor, the capillary pressure introduces distortions of the pores. The elastic modulus $E_{mod}$ of the mesoporous structure is defined as

$$E_{mod} = \frac{p_c}{\frac{D-D_0}{D_0}} \tag{2.2}$$

with the capillary pressure $p_c$, a typical distorted length $D$ and the undistorted length $D_0$. Depending on the relative humidity $RH$, the

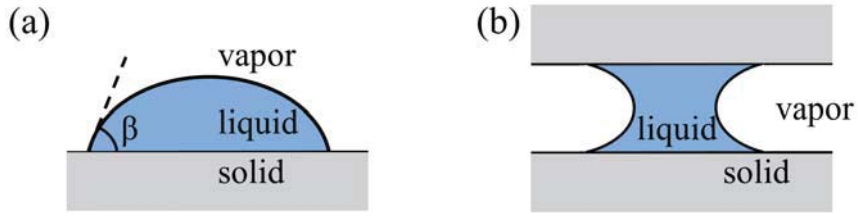


**Figure 2.3:** Principle of wetting: a drop of liquid on a surface with contact angle $\beta$ (a) and a drop confined in a channel (b) are illustrated.

elastic modulus is obtained from the change of typical structural length scales by

$$D = D_0 \left(1 + \frac{RT}{E_{mod} V_L} \ln(RH)\right) \tag{2.3}$$

with the gas constant $R = 8.3144621$ J (mol K)$^{-1}$, temperature $T$ and the molar volume of water $V_L$. This equation is deduced with the use of the Kelvin equation

$$\ln(RH) = \frac{p_c V_L}{RT}, \tag{2.4}$$

as described in reference [23].

### 2.1.2 Hybrid solar cells

Hybrid solar cells combine a hole-conductor like a conjugated polymer with an inorganic electron conductor. All-organic solar cells based on at least one conjugated polymer, often in combination with $C_{60}$-based molecules as electron-conductors, are successful as well [24], with efficiencies above 10% [25]. In both the all-organic solar cells and the hybrid solar cells, typically the absorption takes place mostly in the hole-conducting material. The charge separation is governed by the interface to the electron-conducting material. With the focus on hybrid solar cells in the following, the principle processes are illustrated in the energy level diagram in figure 2.4.

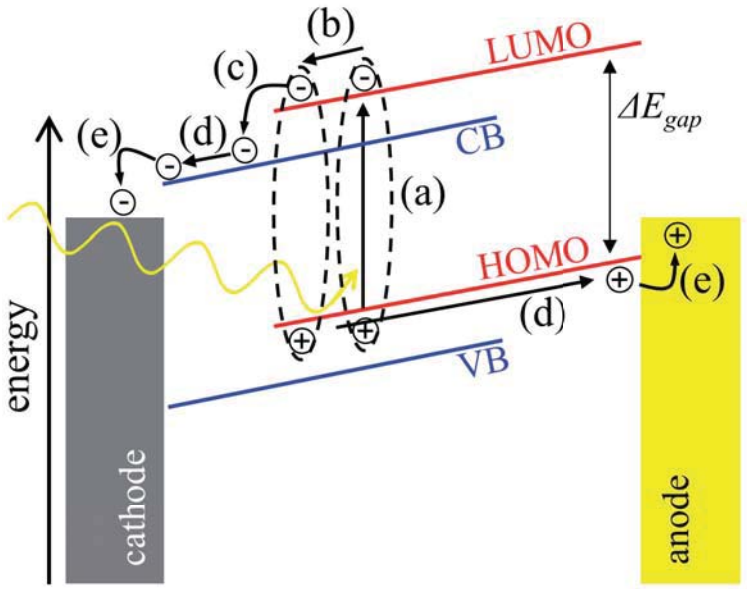


**Figure 2.4:** Energy levels in hybrid solar cell (short cut conditions): the principle processes comprise absorption of a photon with the accompanying excitation of a charge from the HOMO to the LUMO of the polymer and the creation of an exciton (a), the diffusion of the exciton to an interface to titania (b) and the separation of charges (c) through an energy transfer. The electrons are conducted in the conduction band (CB) of titania, the holes in the HOMO of the polymer (d), the charges are extracted at the respective electrodes (e). The valence band (VB) of titania is also indicated.

### Absorption

The absorption of a photon in a conducting polymer leads to the excitation of a charge from the highest occupied molecular orbital (HOMO) to the lowest unoccupied molecular orbital (LUMO) level with an energy gap of $\Delta E_{gap}$. Consequently, only photons with an energy larger or equal to $\Delta E_{gap}$ are absorbed, for light with a wavelength $\lambda$, the speed of light $c_0$ and Planck's constant $h$, the energy needs to be

$$E = \frac{hc_0}{\lambda} \geq \Delta E_{gap}. \tag{2.5}$$

The electronic transitions are much faster than the nuclear motion of the polymers, according to the Franck Condon principle. In case of a tran-

sition to an electronic state with another mean nuclear distance $R_0$, the excitation is to a higher vibrational state, with an overlap of the quantum mechanical wave functions, depicted as straight lines in the diagram in figure 2.5. The absorption of photons with the excitation of charges from one state to another leads to one absorption line. This one peak exhibits a certain width due to the lifetime of the excited state, as the width in time and the width in energy are related through Heisenberg's uncertainty relation [26]. Furthermore, a fine structure of absorption is observed due to the inner structure of the polymer and the polymer crystal, as an excitation occurs also from one molecule to the next [27], depending on how the polymers aggregate. For example, the intrachain interactions in the regular crystal of the hole-conducting polymer poly(3-hexyl-thiophene) (P3HT) lead to additional absorption lines, in addition to the 0-0 vibronic intrachain excitation [28]. For P3HT, the absorption spectrum can be calculated with the weakly coupled H aggregate model [29]. The relation of the 0-0 to the 0-1 absorption line yields the exciton band width $W$ through

$$\frac{A_{0-0}}{A_{0-1}} = \frac{n_{0-0}}{n_{0-1}} \left( \frac{1 - 0.24W/E_p}{1 + 0.073W/E_p} \right) \tag{2.6}$$

with the ratio of refractive indices $n_{0-0}/n_{0-1} \approx 0.97$ and the phonon energy of the main oscillator coupled to the electronic transition, $E_p = 0.18$ eV [29]. From the observed relation of the absorption lines, the ratio of unaggregated and aggregated P3HT can be determined [29, 30, 31]. To determine this ratio and consequently the degree of crystallinity in the P3HT film, the ratio of the area calculated from the weakly coupled H aggregate model to the area of the difference to the measured data is calculated. The part of the spectrum that cannot be described with the model is attributed to unaggregated polymer. This attribution was confirmed by measurements of a dilute P3HT solution, where all P3HT chains are unaggregated [30].

In general, an overlap of the solar spectrum and absorption spectrum is highly important for the solar cell efficiency, as much solar light as possible needs to be absorbed in efficient solar cells. To absorb most of the light, typically 200 to 300 nm of the absorbing polymer are sufficient.

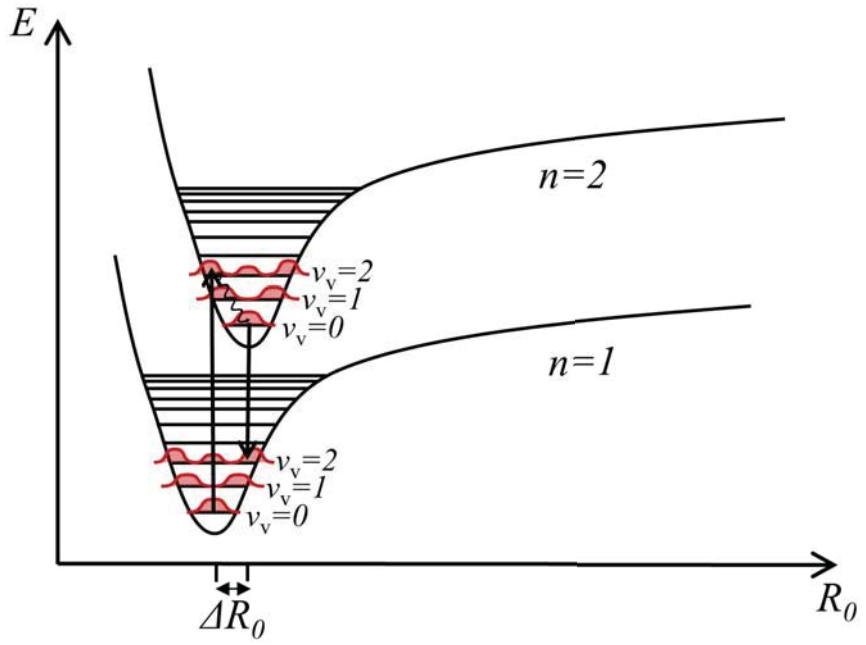


**Figure 2.5:** Franck Condon principle: the energies $E$ of the first electronic state $n = 1$ and the second electronic state $n = 2$ are indicated as a function of the nuclear distance $R_0$, together with the energy levels of different vibrational states $\nu_v$. The square of the wave functions for the first three vibrational states are also sketched. An electronic transition is much faster than the nuclear motion, resulting in the transitions indicated by the straight arrows. The additional internal relaxations are radiationless (wavy arrow).

## Diffusion of excitons

The excitation of charges leads to the creation of bound electron-hole pairs, so-called excitons. The energy of the excitons can be calculated with quantum mechanics just as for a simple hydrogen atom or a positronium atom (the bound pair of an electron and a positron), with an adjusted force between the positive and the negative charge due to the surrounding atoms. In case of a weak interaction, the excitons are called Mott-Wannier exciton and have a large mean size of several atomic distances. Frenkel excitons are strongly bound excitons and have a small size, often located on one atom [32]. A schematic representation of the two types of excitons is shown in figure 2.6. In practice, all types of ex-

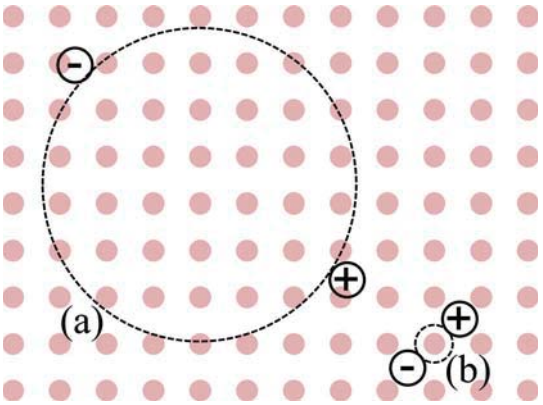


**Figure 2.6:** Definition of excitons: a weakly bound Mott-Wannier exciton (a) and a strongly bound Frenkel exciton (b) are shown in the sea of atomic kernels depicted in light red.

citons between the two extremes of Mott-Wannier excitons and Frenkel excitons exist as well. The exciton state in the energy diagram lies at $E_n$, below the LUMO level of the polymer. The energy can be calculated from the elementary charge $e$, the reduced Planck constant $\hbar = {}^{h}/_{2\pi}$ and the dielectric constant $\varepsilon$ of the material through

$$E_n = E_{gap} - \frac{\mu e^4}{2\hbar^2 \varepsilon^2 n^2} \tag{2.7}$$

with the effective mass $\mu^{-1} = m_e^{-1} + m_h^{-1}$ of electrons with mass $m_e$ and holes with mass $m_h$ in the case of Mott-Wannier excitons. In the case of Frenkel excitons, the energy depends also on the wave vector [32]. In the case of inorganic semiconductors the typical binding energies of excitons are all in the range of thermal energy ($k_B T = 25$ meV for room temperature, with Boltzmann's constant $k_B$ and temperature $T = 20$ °C). For example in silicon an exciton binding energy of 14.7 meV is observed, Ge and GaAs both show exciton binding energies of around 4.2 meV. As noted above, in the investigated organic systems, binding energies of excitons of around 0.5 eV are observed due to the small dielectric constant $\varepsilon$. With around 0.5 eV the binding energies are much higher than the thermal energy [14]. Due to the large binding energy of the excitons, the thermal energy is not sufficient to separate the charges and the excitons need to diffuse to an interface with the electron-conducting material. In the polymer phase, the exciton diffusion takes place via several energy transfer processes. Consequently, the process can be understood as a random walk of the exciton via hopping

from one polymer site to the next. Due to the random nature of the diffusion, the overall exciton diffusion length $l_e$ is a lot smaller than the totally covered distance, with

$$l_e = \sqrt{2dD_e\tau_e}, \tag{2.8}$$

for diffusion in a material with dimensionality $d$, exciton diffusion coefficient $D_e$ and exciton lifetime $\tau_e$, which is of the order of ns [33]. Typical exciton diffusion lengths in hole-conducting polymers are around 10 nm [33, 34]. The limited diffusion length is a major limiting process in the case of hybrid solar cells, as recombination of the excitons occurs before separation when the pathway of an exciton to the interface is too long. Therefore, the nanostructure of the hybrid solar cells needs to provide a distance between interfaces of maximum 20 to 30 nm for an efficient charge separation.

### Charge separation

Due to an altered energy at the interface, the excitons can be separated. The charge separation at the polymer-titania interface takes place via an energy transfer [34], as depicted in figure 2.7. An efficient charge separation process requires an overlap of the energy levels of the hole-conducting polymer and the bands of titania, as indicated in figure 2.7. From organic photovoltaics, it is known that the energy transfer can take place either via a trivial energy transfer process or via a Förster transfer. In the case of a trivial energy transfer process, the donor material emits a photon by fluorescence, this photon is reabsorbed in the acceptor material and creates a new excitation there. The trivial energy transfer process is dominant for distances larger than 10 nm. The Förster transfer is also known as fluorescence resonance energy transfer (FRET). It was originally developed for diluted dye molecules but can be extended to conjugated polymer systems. The radiationless energy transfer of FRET from the donor material to the acceptor material takes place through dipole-dipole coupling. The emission spectrum of the donor has to overlap with the absorption spectrum of the acceptor.

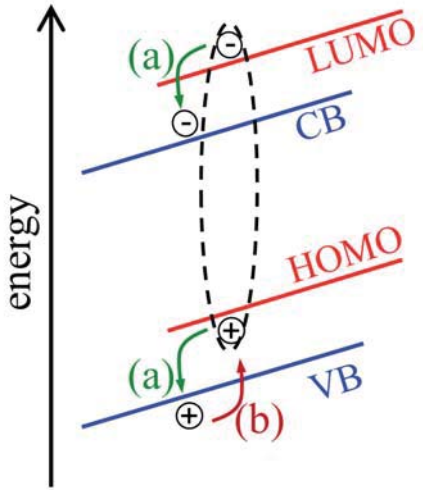


**Figure 2.7:** Energy transfer: the HOMO and LUMO levels of the donor polymer and the valence and conduction bands of titania are depicted. The exciton, indicated by the dashed ellipse, is dissociated via the energy transfer (a) from the polymer to titania, followed by a charge transfer (b) of the hole from titania back to the polymer.

Then, the transfer rate is maximum for parallel dipoles. With these conditions, the Förster transfer is most important for short distances below 10 nm. After the energy transfer with the subsequent charge transfer of the hole back to the hole-conducting HOMO level, the separated charges reside on the different materials.

Regarding the lifetime of the hybrid solar cells, the hole-conducting material poses typically the limit, as the polymer oxidizes in contact with air. Furthermore, oxidizing contacts limit the lifetime of organic solar cells, which is prevented in the case of gold or silver contacts instead of aluminum contacts. The organic hole-conducting materials degrade also in UV. In the case of titania as electron conductor, the UV light is already absorbed before entering the polymer. In that case, the lifetime of the solar cell is increased by a decreased aging of the polymer.

### 2.1.3 Solid-state dye-sensitized solar cells

Dye-sensitized solar cells (DSSCs) with an electrolyte as hole-conductor have been investigated since the 1990s [35, 36, 37], and are already applied in the meantime. Due to sealing problems with the liquid electrolyte, which is typically iodine based and consequently highly corrosive, the replacement of the electrolyte with a solid hole-conductor is highly interesting. The principle energy diagram is the same for both types of DSSCs, but the regeneration happens via the hole-conducting

material and not the electrolyte in the case of a solid-state DSSC (ss-DSSC). The energy levels with the dye states are depicted in figure 2.8, following [18] and [37].

### Absorption

In ssDSSCs, the light is absorbed in the dye that covers the titania with a monolayer. Typically, the dyes used in DSSCs and ssDSSCs are ruthenium-based [38]. However, the search for all-organic dyes is ongoing [39]. Only photons are absorbed that have an energy equal to or larger than the energy gap $\Delta E_{gap}$ between the ground state of the dye $S$ and the excited state $S^*$, as in the case of absorption in a polymer, see equation (2.5). The absorption in the dye also follows the Franck Condon principle, see figure 2.5. The subsequent evolution of the excited state in the dye is summarized in figure 2.9 [40]. The absorption with an excitation of charges from the singlet ground state to the excited singlet state takes place in $10^{-15}$ s, internal conversion to a singlet state with a lower energy is also fast with a typical time of $10^{-14}$ up to $10^{-13}$ s. The radiative fluorescence process takes place in $10^{-9}$ up to $10^{-5}$ s. Intersystem crossing to a triplet state, which is only allowed in case the vibrational states overlap, happens typically in $10^{-6}$ s. Phosphorescence is a slow process with $10^{-5}$ up to $10^{-3}$ s, due to the long lifetime of the triplet state. In addition to the radiative decay via fluorescence or phosphorescence, also internal and external radiationless conversion are possible [40]. For an efficient solar cell, the charge separation process needs to be faster than all the decay processes. This is the case for the ruthenium based dye used in the present thesis [41]. Furthermore, as much of the solar light needs to be absorbed as possible. To that end, enough of the dye needs to be present in the solar cells.

The most problematic aspect of the dye lies in the bleaching with time. Thereby, DSSCs have a limited lifetime and the synthesis of new dye materials also focuses on the stability of the dye under illumination.

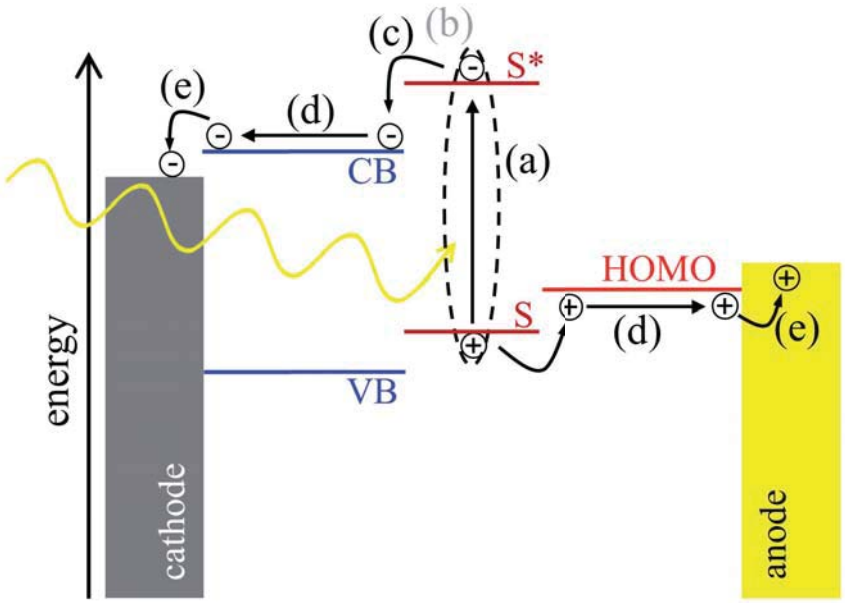


**Figure 2.8:** Energy levels in ssDSSC (omitting the band bending): the principle processes comprise absorption, charge separation, charge transport and charge extraction. The absorption of a photon leads to the excitation of charges from the ground state $S$ to the excited state $S^*$ in the dye (a). The electron is injected into the CB of titania (c) without any migration of the excited state (consequently, (b) is omitted). The dye is regenerated by the hole-conducting polymer, the charges are transported to the respective electrodes in the CB of titania and in the HOMO level of the polymer (d). Finally, the charges are extracted at their respective electrodes (e).

### Charge separation

The excited charges in the dye molecules are separated and injected into titania via an electron transfer [37]. The simple principle of the charge transfer (electron transfer) is depicted in figure 2.10(a) [34]. An overlap of the dye states and the titania state has to be given for an efficient charge transfer. The overlap is due to binding of dye to the titania surface. In Gerischer's model [15], in reality not only Franck Condon energy levels of the dye molecules are present, but all the energy levels follow a Gaussian distribution around the most probable state. This Gaussian distribution is due to thermal fluctuations in the interaction

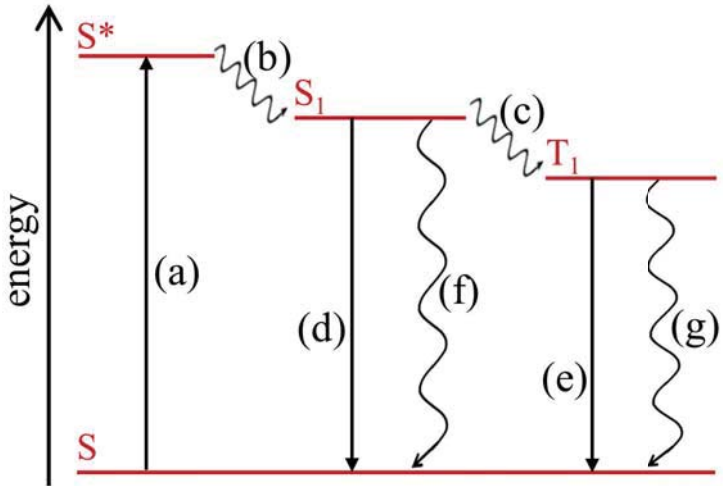


**Figure 2.9:** Evolution of excited state in dye: the ground state $S$, the excited singlet states $S^*$ and $S_1$ and the excited triplet state $T_1$ are shown without the vibrational states that exist for each electronic state in addition. After absorption (a), internal conversion (b) and intersystem crossing (c) are possible, leading to fluorescence (d) and phosphorescence (e) or internal or external radiationless conversions (f, g) (figure adapted from [40]).

with the surrounding and thermal excitation of vibrations and rotations. For example, in the case of a molecule acting as a donor, the distribution function $W_{\mathrm{don}}$ as a function of the energy $E$ can be written as

$$W_{\mathrm{don}}(E) = \frac{1}{\sqrt{4\pi k_B T L_{\mathrm{don}}}} \exp\left(-\frac{(E - E_{\mathrm{don}})^2}{4 k_B T L_{\mathrm{don}}}\right) \tag{2.9}$$

with the reorganization energy of the donor state $L_{\mathrm{don}}$ and the most probable electron transfer energy level $E_{\mathrm{don}}$. Again, the thermal energy is given by $k_B T$ with Boltzmann's constant $k_B$ and the temperature $T$. In figure 2.10(b), the valence and conduction bands (VB and CB) of titania are schematically depicted as occupied and unfilled bands, the dye states are shown as their Gaussian distributions. The rate of the electron transfer $j_{\mathrm{don}}$ from the donor material (the dye) to titania can be written as

$$j_{\mathrm{don}} = B_{\mathrm{don}} c_{\mathrm{don}} \int_{-\infty}^{\infty} \chi_{\mathrm{don}}(E) W_{\mathrm{don}}(E) D_{\mathrm{vac}}(E) \mathrm{d}E \tag{2.10}$$

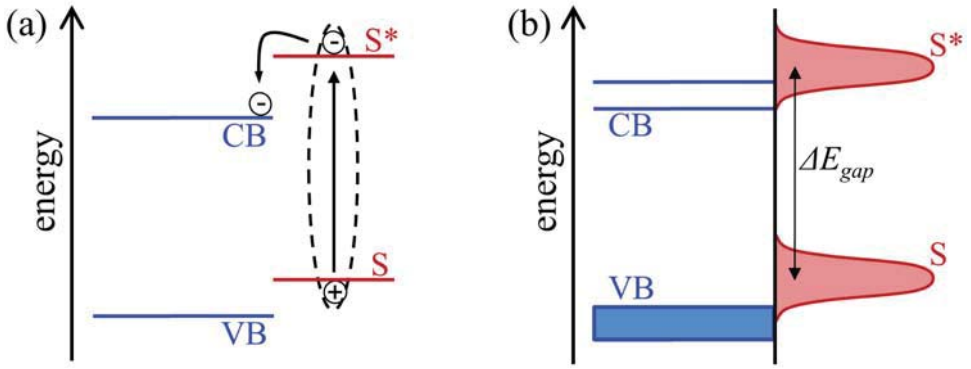


**Figure 2.10:** Electron transfer and Gerischer's model: the excited state S* and the ground state S of the dye and the valence and conduction bands of titania are depicted. The exciton, indicated by the dashed ellipse, is dissociated via the electron transfer from S* to the conduction band of titania (a). In Gerischer's model, the states of the dye follow a Gaussian distribution (b), due to the overlap with the vacant CB of titania (indicated by the empty band), the electron transfer is possible. The injection of an electron from the occupied VB of titania (indicated by the filled band) to the dye is unlikely due to the missing overlap.

with constants $B_{\text{don}}$ and $c_{\text{don}}$, the electron transition probability $\chi_{\text{don}}$ and the density of vacant electron states in the titania $D_{\text{vac}}$ [15]. In general, also the electron transfer from the VB of titania to the ground state of the dye is possible. In case of no overlap of these levels, as depicted in figure 2.10(b), the electron transfer is a highly efficient process with a very high quantum efficiency. However, the electron injection overpotential is of the order of 100 to 150 mV and the dye regeneration overpotential is lower in the case of ssDSSCs than in iodide based DSSCs, but still around 200 mV. Therefore, the maximum theoretical efficiency is limited to 22%. The overpotentials result in a decrease of the open circuit voltage [42].

The electron transfer also follows the Franck Condon principle and the electronic transition is much faster than the atomic movement. Therefore, after the electron transfer, the dye molecule and the surrounding need to reorganize.

As the charge separation process is only effective for a monolayer of dye, nanostructured titania is necessary to supply the surface necessary to provide enough dye to absorb enough light. An active layer thickness of 2 µm is optimum for the successful application in ssDSSCs [43].

## 2.2 Polymer basics

As noted above, two types of polymers are used in the present thesis, block copolymers to template the titania nanostructure and hole-conducting polymers that constitute a part of the active material in the solar cells. The basics of polymer physics necessary to understand the involved processes are discussed along with block copolymer basics in section 2.2.1. Remarks on crystallization and phase separation in polymer blends are also given along with the micro-phase separation in block copolymers. Electrically conducting polymers are discussed in section 2.2.2, including a short discussion of the band gap in polymers with a conjugated backbone, the types of charge carriers and hopping transport.

### 2.2.1 Block copolymers

Before the discussion of block copolymers, a few remarks are given on polymer basics. A polymer consists of macromolecules, which in turn consist of many copies of the same basic repeating unit, the so-called monomer. The monomers are covalently bound to each other. Molecules in general are classified according to their molecular mass $M_w$ as

- micro-molecules: $M_w < 1000$ g mol$^{-1}$
- oligomers: $(1000 \leq M_w \leq 10000)$ g mol$^{-1}$
- polymer macromolecules: $M_w > 10000$ g mol$^{-1}$.

The different terms used to describe polymers are defined by the IUPAC (International Union of Pure and Applied Chemistry) as listed in reference [44].